Atmos. Chem. Phys. Discuss., 5, 5909–5934, 2005
www.atmos-chem-phys.org/acpd/5/5909/
SRef-ID: 1680-7375/acpd/2005-5-5909
European Geosciences Union

Atmospheric Chemistry and Physics Discussions

Effect of smoke on the transmissivity of photosynthetically active radiation inside the canopy

M. Yamasoe[1], C. von Randow[2], A. Manzi[3], J. Schafer[4,5], T. Eck[5,6], and B. Holben[5]

[1]Instituto de Astronomia, Geofísica e Ciências Atmosféricas da Universidade de São Paulo, Rua do Matão, 1226, São Paulo, SP, 05508-090, Brazil
[2]Wageningen University and Research Centre, Wageningen, The Netherlands
[3]Instituto Nacional de Pesquisas da Amazônia, Av. André Araújo, 2936, Manaus, AM, Brazil
[4]Science Systems and Applications Inc., Greenbelt, MD, USA
[5]NASA Goddard Space Flight Center, Greenbelt, MD, 20771, Biospheric Sciences Branch, Code 614.4, USA
[6]University of Maryland-Baltimore County, Goddard Earth Sciences/Technology Center, USA

Received: 6 July 2005 – Accepted: 19 July 2005 – Published: 12 August 2005

Correspondence to: M. Yamasoe (akemi@model.iag.usp.br)

Abstract

Biomass burning activities emit high concentrations of aerosol particles to the atmosphere. Such particles can interact with solar radiation, decreasing the amount of light reaching the surface and increasing the fraction of diffuse radiation through scattering processes. This work reports results from photosynthetic active radiation (PAR) and aerosol optical depth (AOD) measurements conducted simultaneously at Reserva Biológica do Jaru (Rondonia State, Brazil) during LBA/SMOCC (Large-Scale Biosphere-Atmosphere Experiment in Amazonia/ Smoke, Aerosols, Clouds, Rainfall, and Climate) and RaCCI (Radiation, Cloud, and Climate Interactions in the Amazon during the Dry-to-Wet Transition Season) field experiments from 15 September to 15 November 2002. AOD values were retrieved from an AERONET (Aerosol Robotic Network) radiometer, MODIS (Moderate Resolution Spectroradiometer) and a portable sunphotometer from the United States Department of Agriculture-Forest Service. Daily mean downward PAR irradiance at the top of canopy was reduced by up to 50% due to the smoke aerosol particles. This radiation reduction affected turbulent fluxes of sensible and latent heats at the surface, observed particularly for high values of aerosol optical depth. The increase of aerosol optical depth also enhanced the transmission of photosynthetic active radiation inside the canopy. This result was a consequence of enhanced availability of diffuse radiation due to light scattering by the aerosol particles. A complex relationship was identified between light availability inside the canopy and net ecosystem exchange (NEE). The results showed that the increase of aerosol optical depth corresponded to an increase on CO_2 exchange, indicating more CO_2 uptake by the vegetation. However, for a higher AOD value, the corresponding NEE was lower than for intermediate values. Further studies are needed to better understand these findings, which were reported for the first time for the Amazon region under smoky conditions.

1. Introduction

Aerosol particles are well known to affect the climate system by interacting with solar radiation through direct and indirect processes. The direct process involves absorption and scattering of solar radiation. While scattering affects climate reflecting part of the available radiation back to space and thus cooling the surface, absorption of solar radiation can cool the surface and heat the atmosphere. Both effects of cooling the surface and heating the atmosphere can stabilize the atmosphere by changing its thermodynamic profile. If less energy is available at surface level, turbulent fluxes are inhibited with less evaporation of water vapor from vegetation and water bodies, implying in a drier lower atmosphere. If the atmosphere is more stable and drier, less clouds can be formed, a named semi-direct aerosol effect (Koren et al., 2004). The indirect process is coupled to the cloud condensation nuclei property of aerosol particles, whose excess can change cloud properties and lifetime in the atmosphere (Twomey, 1977; Kaufman and Nakajima, 1993; Kaufman and Fraser, 1997; Andreae et al., 2004). Recently another consequence of the aerosol direct effect on solar radiation has been brought under investigation, namely, the effect on the yields of crops due to a reduction in the photosynthetic active radiation (PAR, 400 to 700 nm) reaching the Earth's surface and the increase of its diffuse fraction (Chameides et al., 1999; Cohan et al., 2002; Gu et al., 2002, 2003).

Particles with diameters of 0.1 to 1.0 μm scatter light most efficiently in the wavelengths used for photosynthesis. During the dry season in the Amazon region, large amounts of such particles are emitted from biomass burning activities to the atmosphere (Andreae et al., 1991; Kaufman et al., 1998; Yamasoe et al., 2000). Measurements performed in the region showed significant reduction of downward solar total and photosynthetic active irradiance at the surface (Schafer et al., 2002; Procopio et al., 2004; Eck et al., 1998). On the other hand, diffuse fraction of PAR can increase from 19% with a clear atmosphere up to 80% under heavy smoke conditions (Yamasoe et al., 2005[1]). The purpose of the present work is to assess the effect of the smoke layer on the transmission of PAR inside the canopy in a tropical rainforest in the Amazon region and investigate the possible consequences of this effect to the vegetation.

2. Experimental setup and methodology

The measurements were performed as part of SMOCC (Smoke, Aerosols, Clouds, Rainfall, and Climate) and RaCCI (Radiation, Cloud, and Climate Interactions in the Amazon during the Dry-to-Wet Transition Season) field experiments at a 60-m high micrometeorological tower located at Reserva Biológica Jaru, hereafter called Rebio Jaru (10°04.71′ S, 61°56.0′ W). The tower is surrounded by tropical rainforest vegetation with mean canopy height of 30–35 m, with some trees as high as 45 m. Although the tower is settled in a governmental protected area, as mentioned by Andreae et al. (2002) landless people developed small-scale slash and burn activities in the area. During the field experiment it was possible to see fires and smoke nearby from the top of the tower. Additional information about the site can be obtained from Andreae et al. (2002) and Von Randow et al. (2002).

PAR downward irradiance measurements were carried out at seven different heights above surface: from the top of the canopy at 39 m, 30, 25, 19, 15, 10 and 5 m. Energy sensors SKE 510 from Skye Instruments were used. The sensors were mounted at the faces to the north, east and west of the tower on 4 m-long-aluminum poles. Other six sensors measured reflected PAR irradiances at 39 and 30 m at the same three faces. Other four sensors were setup at about 1 m from the surface, also measuring downward PAR irradiance. Measurements were performed every minute from 15 September up

[1]Yamasoe, M. A., Plana-Fattori, A., Corrêa, M. P., Garcia, M. P., Dubuisson, P., Holben, B. N., Schafer, J., Eck, T., and Artaxo, P.: Measurement of global and direct-normal incidence PAR irradiance under smoky conditions in the Amazon Basin, Atmos. Chem. Phys. Discuss., to be submitted, 2005.

to 15 November 2002.

Aerosol optical depth was retrieved from a Cimel radiometer from AERONET (Aerosol Robotic Network) (Holben et al., 1998) mounted at a second tower located about 800 m from the main tower. Aerosol optical depth from a portable sunphotometer (hazemeter), from USDA-FS (United States Department of Agriculture-Forest Service) which was operated at the site, as part of a regional network spread over states of Rondonia and Acre was also analyzed. Additional information on the hazemeters (description, operation and calibration), can be accessed at http://s2k.gsfc.nasa.gov/html_pages/groups/atm/hazemeter_doc.html. Finally retrievals from MODIS (Moderate Resolution Spectroradiometer) (Kaufman et al., 1997; Remer et al., 2005) aboard Terra (about 10:30 h LT overpass) and Aqua (about 13:30 h LT overpass) satellites were also used in this study, since the AERONET radiometer was not available at the end of the sampling period due to instrumental problems. For the period while AERONET instrument was operating simultaneously with the hazemeter and MODIS, aerosol optical depth retrieved from the hazemeter measurements and from MODIS was quality assured with AERONET data, considered our reference instrument. Results from the hazemeter and MODIS were corrected, since hazemeter tended to overestimate AOD as compared to AERONET and since MODIS aerosol optical depth was retrieved at wavelength 0.550 μm while both AERONET and the hazemeter values used in this manuscript are for 0.500 μm.

Latent, sensible and CO_2 fluxes were determined from fast response wind velocity, temperature, humidity and CO_2 concentration measurements performed with a 3-D sonic anemometer (Solent 1012R2, Gill Instruments, UK) and an infrared gas analyzer (LI-6262, LICOR, USA) installed at 62.7 m height. The fluxes were estimated using the eddy covariance method. The fluctuations of the variables were calculated by subtracting 60-min block average values from the instantaneous measurements. Also, two rotations were applied to align the coordinate frame with the mean streamlines and to force the mean vertical component to zero. A detailed description of the eddy covariance system and flux calculations is provided by Von Randow et al. (2004). An estimate of net ecosystem exchange (NEE) was performed as the sum of the fluxes measured at the top of the tower and the change in storage of CO_2 in the layer below. To quantify this change in storage, an empirical model was proposed by Von Randow et al. (2004) and is based on the amount of turbulence observed during the preceding night.

AERONET retrievals of size distribution and complex refractive index (according to an inversion model developed by Dubovik and King, 2000) were also used to develop an aerosol optical model at PAR spectral range. Refractive index was linearly interpolated in the PAR region in bin size intervals of 0.025 μm and input in a Mie code developed by Wiscombe (1980) together with size distribution to calculate single scattering albedo (ϖ_0), asymmetry factor (g) and extinction efficiency (Q_{ext}). The optical model was used as input in the radiative transfer code SBDART (Santa Barbara DISORT Atmospheric Radiative Transfer) (Ricchiazzi et al., 1998) to simulate downward global PAR irradiance at the top of the canopy.

3. Results

Table 1 presents the calculated parameters of the optical model for biomass burning aerosol particles. The extinction efficiency at the table is normalized at 0.55 μm. The results are similar to Procópio et al. (2003) values. The authors analyzed data from two AERONET radiometers located 700 km apart in the southern Amazon Basin, Alta Floresta (09°55′ S, 56°00′ W) and Abracos Hill (10°45′S, 62°21′ W). Procopio et al. (2003) reported mean values of 0.67±0.01 and 0.56±0.02, respectively at 0.44 and 0.67 μm, for asymmetry factor. Extinction efficiency from this work presents a slightly lower spectral dependence when compared to Procopio and co-authors results. Figure 1 shows a comparison of single scattering albedo from Mie calculations from this work and mean values retrieved from AERONET. Vertical bars indicate the variability of AERONET results. Mean values from the 12 optical models proposed by Procópio et al. (2003) are also shown. Chand et al. (2005) retrieved single scattering albedo of about 0.92±0.02

(at 545 nm) from in situ measurements of linear scattering and absorption coefficients performed at Fazenda Nossa Senhora Aparecida during SMOCC (same location of Abracos Hill AERONET site) field campaign, for submicron particles (with diameter lower than 1.5 μm) and dry ambient conditions (relative humidity of about 40%).

Daily mean values of aerosol optical depth at 500 nm are presented in Fig. 2. As discussed previously both hazemeter and MODIS results were corrected according to AERONET results, in order to extend the time series for the entire field campaign, since the radiometer from AERONET was not available all the time. Mean values higher than 2.0 were observed at the beginning of the sampling period, indicating a very polluted atmosphere. Gradually AOD decreased at the site mostly due to rainfall, reaching mean values of 0.35 to 0.40 by the end of the experiment.

This smoke layer affected downward PAR irradiance measured at the top of canopy as can be observed in Fig. 3. For each AOD value, it is shown a measured (diamond) and calculated (circle) daily mean PAR irradiance value (representing data from sunrise to sunset). Open symbols illustrated all data, except days classified as completely overcast, or when AOD retrievals were not available, and solid symbols correspond to cases not significantly affected by clouds. For higher AOD values, less incident global PAR was measured. A decrease of up to 50% could be observed. A correlation coefficient of −0.39 between PAR and AOD was obtained considering all data which also included cloudy days. Excluding days on which cloud cover affected more than 10 percent of the data, a correlation coefficient of −0.96 was obtained (cases presented as solid diamonds in Fig. 3). The methodology describing how the cloudy days were excluded will be discussed further ahead in this text.

Analyzing the effect of smoke on the transmission of PAR through the canopy, an increase of transmittance was observed with the increase of AOD, as shown in Fig. 4. The estimation of transmittance was obtained normalizing daily mean downward irradiance measured at one particular level for the one measured at the top of the canopy (at 39 m). Since aerosol particles in the atmosphere increase the availability of diffuse radiation, the result presented in Fig. 4 indicates a more efficient penetration of PAR inside the canopy in the presence of the smoke layer.

As mentioned previously, downward PAR irradiance at the top of the canopy was attenuated due to the presence of the smoke layer. As expected, if less radiation reaches the surface, there is a decrease in turbulent fluxes. This effect was observed in the dataset including cloudy cases (not shown). In order to investigate only the effect of the smoke layer, days classified as cloud-contaminated were excluded from the analysis. Figure 5 illustrates results of the numerical calculation of downward PAR irradiances at the surface performed with SBDART radiative transfer code. The calculations were performed at the same 1-min time step of the measurements. In Fig. 5a, the difference between measured and calculated daily mean downward irradiance in the PAR spectral region was −3.1%. Notice that since numerical calculations were performed with no cloud information, but only with aerosol optical properties, for days when clouds were presented, calculations values would be always higher than measured. Since the relative difference considers measured minus calculated irradiances, the result is always negative. Figure 5b shows a cloud-contaminated example, for which the difference between measured and modeled downward PAR was −50%. Cases for which the absolute difference between calculated and measured daily mean values was higher than 10% were classified as cloud-contaminated. Notice that even on 20 September, case shown in Fig. 5a, there were some scattered clouds around 3 p.m. (UTC), accounting for the 3% observed difference. Unfortunately, the evaluation of the smoke effect only is very difficult. For the sampling period, which comprised two months of measurements during the dry season, clouds were always present (due to a meteorological characteristic of the region). In this analysis we tried to minimize the influence of clouds by excluding cases for which the difference between measured and calculated downward PAR was higher than 10%.

Analyzing Fig. 6, where only cases with low cloud influence were considered, we observe that attenuation of solar radiation at the surface due to smoke layer is strong enough to interfere on turbulent fluxes. As aerosol loadings increased, quantified as AOD, it was possible to observe a decrease in turbulent fluxes. A reduction of about

ACPD
5, 5909–5934, 2005

20% was observed for latent heat as AOD varied from 0.5 to 2.5 and of more than 50% in the case of sensible heat flux. No similar results could be found in the literature in order to compare to the results reported here. For low AOD values, however, data is more scattered suggesting that other processes, rather than solar radiation attenuation, are responsible for the variability of turbulent fluxes, such as the temperature or soil moisture conditions, or even local circulations as discussed by Von Randow et al. (2002).

Finally, there is no clear evidence on the influence of the aerosol particles from biomass burning on CO_2 flux, particularly due to the low number of analyzed cases (cloudless cases only). From Fig. 7 it is possible to observe high variability on CO_2 flux for low AOD values, which was also observed for energy fluxes. An increase (more negative flux, indicating more CO_2 uptake by vegetation) for intermediate values and a decrease for high AOD values can be observed in the figure. A quite similar behavior is observed for NEE. Niyogi et al. (2004) also observed an increase of CO_2 flux for AOD varying from 0.1 to 0.8. For a broadleaf deciduous forest in Walker Branch, TN, US, they observed an increase from -15 up to about $-24\,\mu\text{mol}\,\text{m}^{-2}\text{s}^{-1}$ for that AOD range. According to their results, C4 vegetation presented the largest sensitivity, C3 crops/grasslands less and trees from the deciduous forest moderate sensitivity for aerosol on CO_2 flux. Actually, grassland sites presented an opposite response with a decreasing CO_2 flux as aerosol loading increased. They hypothesized this difference to the distinct canopy architecture. Unfortunately, aerosol loading at their studied sites was not as high as observed in the Amazon region during the burning season, thus it was not possible to conclude if the reduction on CO_2 flux observed in this work was caused by any instrumental problem or a real aerosol effect. It must be stressed that during biomass burning season daily mean AOD reaches values higher than one frequently in the Amazon region, and eventually over 3, as observed in Fig. 8, which presents daily mean AOD from three AERONET sites located in the Amazon region, since 1999. Assuming no instrumental problem occurred, some possible explanations for this behavior are discussed: 1) for intermediate values of AOD, the increase of the diffuse fraction of PAR enhances photosynthetic activities up to a level where the amount of global radiation is too low due to this same smoke layer, inhibiting photosynthesis; 2) if high AOD inhibits the energy fluxes, due to a stabilizing effect of the atmosphere, in principle CO_2 flux might decrease due to this same effect, causing a complex behavior due to the more availability of diffuse radiation and stabilization of the atmosphere; 3) for high AOD, the concentration of aerosol particles or gases such as ozone in the atmosphere is so high that photosynthesis decreases due to metabolic processes in order to protect vegetation from the poisonous effect of any chemical compounds in the atmosphere. As reported by Andreae et al. (2002), ozone concentration at Rebio Jaru during the dry season of 1999 reached values higher than 40 ppb. This threshold defines ozone critical level, according to the Protocol to Abate Acidification, Eutrophication and Ground-level Ozone (http://www.unece.org/env/lrtap/full\%20text/1999\%20Multi.e.pdf). Ozone is a secondary product from vegetation fires.

Comparing CO_2 fluxes from Figs. 7 and 9, it seems that, in fact, hypotheses 1 and 2 are very plausible. Figure 9 shows a scatter plot of CO_2 and NEE fluxes as function of the percentage difference between measured and calculated daily mean PAR irradiance. Data were averaged out in bin intervals of the percentage difference. This percentage was used previously to identify cloud-contaminated days, since calculations were performed with no clouds. Thus if this percentage increases (absolute value), we assumed that cloud cover increases and its effect on solar radiation becomes more important than the aerosol effect. From Fig. 9 it is possible to observe that the same tendency of increasing CO_2 uptake (more negative CO_2 and NEE fluxes) as cloudiness increases (due to enhancement of diffuse radiation) up to a saturating region where the fluxes stabilize at about −7.6 and −11.5 μmol m^{-2}s^{-1} respectively for CO_2 and NEE fluxes. For completely overcast days, maximum daily mean PAR was lower than 141 W m^{-2} and CO_2 and NEE fluxes continued to go down as the availability of PAR was reduced reaching values of −1.4 and −4.4 μmol m^{-2}s^{-1} respectively for CO_2 and NEE fluxes when mean PAR was about 72 Wm^{-2}, as shown in Table 2. The variability of cloud cover in the region during the course of a day is higher than the aerosol one, being more frequent in the afternoon. Depending on cloud type, atmospheric stability can also vary significantly interfering on the fluxes. However, we suspect that hypothesis 3 could also take place as for those cloudy days when NEE flux was lower than $-15\,\mu\text{mol m}^{-2}\text{s}^{-1}$, AOD values were always below 0.5. When the relative difference of PAR was about −0.5, the day when CO_2 flux was $-10.4\,\mu\text{mol m}^{-2}\text{s}^{-1}$presented a mean AOD value of 0.51 (day 293), while when CO_2 flux equaled $-6.5\,\mu\text{mol m}^{-2}\text{s}^{-1}$ AOD was about 1.95 (day 267). It is interesting to notice also that when AOD was 2.5, mean daily PAR reached about $140\,\text{Wm}^{-2}$ (Fig. 3) and NEE flux was $-7.0\,\mu\text{mol m}^{-2}\text{s}^{-1}$ (Fig. 7). For completely overcast days, when similar mean PAR was obtained, NEE ranged from −10 down to $-15\,\mu\text{mol m}^{-2}\text{s}^{-1}$ (Table 2). Obviously AOD is not appropriate to address this local effect, since it represents an atmospheric column integrated quantity and in situ measurements should be performed in order to study this effect. All these speculative discussions reinforce that further investigations in those directions must still be conducted to get a better understanding of the observed behavior. The aerosol loading during the burning season covers large areas not only in the Amazon region but can be long-range transported to other regions thus could affect carbon budget in a rather regional scale, over areas covered by forest, grass, cerrado (a Brazilian savanna type vegetation) and crops like soybean, cotton, sugarcane. Since the effect of aerosol on CO_2 flux depends on the vegetation structure, as reported by Niyogi et al. (2004), the overall effect on the carbon budget is rather non-linear and must still be addressed.

4. Conclusions

The present work showed that high concentrations of aerosol particles in the atmosphere due to biomass burning decrease the amount of global photosynthetic radiation at canopy levels, affecting sensible and latent heat fluxes at the surface. On the other hand, the smoke layer increases the diffuse fraction of PAR, enhancing transmission of radiation inside the canopy. This seems to enhance photosynthetic activity observed as a more negative CO_2 flux, thus indicating a higher CO_2 uptake by the surrounding vegetation. However, for higher AOD values, CO_2 flux and consequently NEE decreased, which could be due to the less availability of PAR or a consequence of a metabolic process to avoid the deleterious effects of some chemical compounds in the aerosol particles or gases such as ozone, a secondary product from biomass burning which could be formed from emissions from the surrounding fires. Cloud effect on CO_2 exchange is also difficult to quantify, since cloudiness can vary significantly during the course of a day introducing other complexities in the system.

During dry season, large areas are affected by aerosol particles from biomass burning activities due to long-range transport. Thus, the observed effect of the smoke layer on carbon flux and NEE, discussed in this manuscript for the first time for the Amazon region, can have significant implications on the carbon budget. Laboratory studies using photosynthesis chamber, other field campaigns and modeling efforts are planned to improve our understanding of the effect of aerosol particles from biomass burning on the carbon budget.

Acknowledgements. This work was carried out within the frame work of the Smoke, Aerosols, Clouds, Rainfall, and Climate (SMOCC) project, a European contribution to the Large-Scale Biosphere-Atmosphere Experiment in Amazonia (LBA). It was financially supported by the Environmental and Climate Program of the European Commission (contract N° EVK2-CT-2001-00110 SMOCC), the Max Planck Society (MPG), the Fundação de Amparo à Pesquisa do Estado de São Paulo, grants 2001/08574-9 and 2001/06908-7 and the Conselho Nacional de Desenvolvimento Científico e Tecnológico, grants 301151/01-6, 306085/2003-8 and Instituto do Milênio LBA, grant 62.0056/01-0. We thank all members of the LBA-SMOCC and LBA-RACCI Science Teams for their support during the field campaign, especially A. C. Ribeiro, M. A. L. Moura, J. von Jouanne and staff from AERONET. M. Yamasoe acknowledges J. C. Thomaz Jr., J. Mello, J. Martins and staff from Laboratório de Instrumentação Meteorológica/Centro de Previsão do Tempo e Estudos Climáticos (LIM/CPTEC) for support during the field campaign, W. M. Hao for providing hazemeter data, A. A. de Souza for hazemeter operation, K. C. Ng, A. L. Bonini and H. R. Rocha for support on the experimental setup project and A. Correia for revising this manuscript.

References

Andreae, M. O.: Biomass burning: Its history, use and distribution and its impact on environmental quality and global climate, in: Global Biomass Burning: Atmospheric, Climatic and Biospheric Implications, edited by: Levine, J. S., MIT Press, MA, 3–21, 1991.

Andreae, M. O., Artaxo, P., Brandão, C., Carswell, F. E., Ciccioli, P., da Costa, A. L., Culf, A. D., Esteves, J. L., Gash, J. H. C., Grace, J., Kabat, P., Lelieveld, J., Malhi, Y., Manzi, A. O., Meixner, F. X., Nobre, A. D., Nobre, C., Ruivo, M. d. L. P., Silva-Dias, M. A., Stefani, P., Valentini, R., von Jouanne, J., and Waterloo, M. J.: Biogeochemical cycling of carbon, water, energy, trace gases, and aerosols in Amazônia: The LBA-EUSTACH experiments, J. Geophys. Res., 107(D20), 8066, doi:10.1029/2001JD000524, 2002.

Andreae, M. O., Rosenfeld, D., Artaxo, P., Costa, A. A., Frank, G. P., Longo, K. M., and Silva-Dias, M. A.: Smoking rain clouds over the Amazon. Science, 303, 1337–1342, 2004.

Chameides, W. L., Yu, H., Liu, S. C., Bergin, M., Zhou, X., Mearns, L., Wang, G., Kiang, C. S., Saylor, R. D., Luo, C., Huang, Y., Steiner, A., and Giorgi, F.: Case study of the effects of atmospheric aerosols and regional haze on agriculture: An opportunity to enhance crop yields in China through emission controls?, Proc. Natl. Acad. Sci. U. S. A., 96, 13 626–13 633, 1999.

Chand, D., Guyon, P., Artaxo, P., Schmid, O., Frank, G. P., Rizzo, L. V., Mayol-Bracero, O. L., Gatti, L. V., and Andreae, M. O.: Optical and physical properties of aerosols in the boundary layer and free troposphere over the Amazon Basin during the biomass burning season, Atmos. Chem. Phys. Discuss., 5, 4373–4406, 2005, SRef-ID: 1680-7375/acpd/2005-5-4373.

Cohan, D. S., Xu, J., Greenwald, R., Bergin, M. H., and Chameides, W. L.: Impact of atmospheric aerosol light scattering and absorption on terrestrial net primary productivity, Global Biogeochem. Cycles 16(4), 1090, doi:10.1029/2001GB001441, 2002.

Dubovik, O. and King. M. D.: A flexible inversion algorithm for retrieval of aerosol optical properties from Sun and sky radiance measurements, J. Geophys. Res. 105, 20 673–20 696, 2000.

Eck, T. F., Holben, B. N., Slutsker, I., and Setzer, A.: Measurements of irradiance attenuation and estimation of aerosol single scattering albedo for biomass burning aerosols in Amazonia, J. Geophys. Res., 103, 31 865–31 878, 1998.

Gu, L., Baldocchi, D., Verma, S. B., Black, T. A., Vesala, T., Falge, E. M., and Dowty, P.

R.: Advantages of diffuse radiation for terrestrial ecosystem productivity, J. Geophys. Res., 107(D6), art. no. 4050, ACL 2–1 to ACL 2–23, 2002.

Gu, L., Baldocchi, D., Wofsy, S. C., Munger, J. W., Michalsky, J. J., Urbanski, S. P., and Boden, T. A.: Response of a deciduous forest to the Mount Pinatubo eruption: Enhanced Photosynthesis, Science, 299, 2035–2038, 2003.

Holben, B. N., Eck, T. F., Slutsker, I., Tanré, D., Buis, J. P., Setzer, A., Vermote, E., Reagan, J. A., Kaufman, Y. J., Nakajima, T., Lavenu, F., Jankowiak, I., and Smirnov, A.: AERONET – A federated instrument network and data archive for aerosol characterization, Remote Sensing of Environ., 66 (1), 1–16, 1998.

Kaufman. Y. J. and Nakajima, T.: Effect of Amazon smoke on cloud microphysics and albedo – Analysis from satellite imagery, J. Applied Meteor., 32, 729–744, 1993.

Kaufman, Y. J. and Fraser, R. S.: Confirmation of smoke particles effect on clouds and climate forcing, Science, 277, 1636–1639, 1997.

Kaufman, Y. J., Tanré, D., Remer, L. A., Vermote, E., Chu, A., and Holben, B. N.: Operational remote sensing of tropospheric aerosol over land from EOS Moderate Resolution Imaging Spectroradiometer, J. Geophys. Res., 102, 17 051–17 067, 1997.

Kaufman, Y. J., Hobbs, P. V., Kirchhoff, V. W. J. H., Artaxo, P., Remer, L. A., Holben, B. N., King, M. D., Ward, D. E., Prins, E. M., Longo, K. M., Mattos, L. F., Nobre, C. A., Spinhirne, J. D., Ji. Q., Thompson, A. M., Gleason, J. F., Christopher, S. A., and Tsay, S.-C.: Smoke, Clouds, and Radiation-Brazil (SCAR-B) experiment, J. Geophys. Res., 103, D24, 31 783–31 808, 1998.

Koren, I., Kaufman, Y. J., Remer, L. A., and Martins, J. V.: Measurement of the effect of Amazon smoke on inhibition of cloud formation, Science 303, 1342–1345, 2004.

Niyogi, D. Chang, H.-I., Saxena, V. K., Holt, T., Alapaty, K., Booker, F., Chen, F., Davis, K. J., Holben, B., Matsui, T., Meyers, T., Oechel, W. C., Pielke Sr., R. A., Wells, R., Wilson, K., and Xue, Y.: Direct observations of the effects of aerosol loading on net ecosystem CO_2 exchanges over different landscapes, Geophys. Res. Lett., 31, L20506, doi:10.1029/2004GL020915, 2004.

Procópio, A. S., Remer, L. A., Artaxo, P., Kaufman, Y. J., and Holben, B. N.: Modeled spectral optical properties for smoke aerosols in Amazonia, Geophys. Res. Lett., 30, 24, 2265–2270. doi:10.1029/2003GL018063, 2003.

Procopio, A. S., Artaxo, P., Kaufman, Y. J., Remer, L. A., Schafer, J. S., and Holben, B. N.: Multiyear analysis of amazonian biomass burning smoke radiative forcing of climate, Geophys. Res. Lett., 31, L03108, doi:10.1029/2003GL018646, 2004.

Remer, L. A., Kaufman, Y. J., Tanré, D., Mattoo, S., Chu, D. A., Martins, J. V., Li, R.-R., Ichoku, C., Levy, R. C., Kleidman, R. G., Eck, T. F., Vermote, E., and Holben, B. N.: The MODIS Aerosol Algorithm, Products, and Validation, J. Atmos. Sci., 62, 947–973, 2005.

Ricchiazzi, P., Yang, S., Gautier, C. e Sowle, D. SBDART: A research and teaching software tool for plane-parallel radiative transfer in the Earth's Atmosphere, Bulletin of the American Meteorological Society, 79 (10), 2101–2114, 1998.

Schafer, J. S., Eck, T. F., Holben, B. N., Artaxo P., Yamasoe, M. A., and Procopio, A. S.: Observed reductions of total solar irradiance by bio-mass burning aerosols in the Brazilian Amazon and Zambian Savanna, Geophys. Res. Lett., 29(17), 1823, doi:10.1029/2001GL014309, 2002.

Twomey, S.: The influence of pollution on the shortwave albedo of clouds, J. Atmos. Sci., 34, 1149–1152, 1977.

Von Randow, C., Sá, L. D. A., Gannabathula, P. S. D., Manzi, A. O., and Arlino, P. R. A.: Scale variability of atmospheric surface layer fluxes of energy and carbon over a tropical rain forest in southwest Amazonia 1. Diurnal conditions, J. Geophys. Res., 107(D20), 8062, doi:10.1029/2001JD000379, 2002.

Von Randow, C., Manzi, A. O., Kruijt, B., Oliveira, P. J., Zanchi, F. B., Silva, R. L., Hodnett, M. G., Gash, J., Elbers, J., Waterloo, M. J., Cardoso, F. L., and Kabat, P.: Comparative measurements and seasonal variations in energy and carbon exchange over forest and pasture in South West Amazonia, Theoretical and Applied Climatology, 78, 5–26, doi:10.1007/s00704-004-0041-z, 2004.

Wiscombe, W.: Improved Mie Scattering Algorithms, Appl. Opt., 19, 1505–1509, 1980.

Yamasoe, M. A., Artaxo, P., Miguel, A. H., and Allen, A. G.: Chemical composition of aerosol particles from direct emissions of vegetation fires in the Amazon Basin: water-soluble species and trace elements, Atmos. Environ., 34, 1641–1653, 2000.

Table 1. Smoke aerosol optical model in the PAR spectral region developed according to AERONET retrievals of size distribution and refractive index and a Mie code.

Wavelength (μm)	ω_0	g	Q_{ext}
0.400	0.9375	0.6966	1.6293
0.425	0.9360	0.6884	1.5005
0.450	0.9343	0.6800	1.3816
0.475	0.9324	0.6714	1.2722
0.500	0.9304	0.6627	1.1724
0.525	0.9282	0.6541	1.0821
0.550	0.9259	0.6457	1.0000
0.575	0.9235	0.6374	0.9255
0.600	0.9209	0.6293	0.8579
0.625	0.9190	0.6204	0.8064
0.650	0.9164	0.6126	0.7497
0.675	0.9136	0.6051	0.6985
0.700	0.9108	0.5978	0.6518

Table 2. Daily mean values of downward photosynthetic active irradiance at the top of the canopy, CO_2 and NEE fluxes and integrated energy fluxes from sunrise to sunset for completely overcast days.

Day	Daily mean PAR (Wm^{-2})	CO_2 flux ($\mu mol\,m^{-2}s^{-1}$)	NEE flux ($\mu mol\,m^{-2}s^{-1}$)	Latent heat flux (MJm^{-2})	Sensible heat flux (MJm^{-2})
298	131.5	−6.89	−9.94	3.47	0.57
303	89.3	−7.30	−8.86	3.96	−0.18
309	101.3	−9.68	−12.74	4.22	1.85
310	134.9	−10.71	−15.31	5.18	1.32
312	72.0	−1.36	−4.42	3.70	0.10
314	140.1	−7.82	−10.87	7.00	2.00

ACPD
5, 5909–5934, 2005

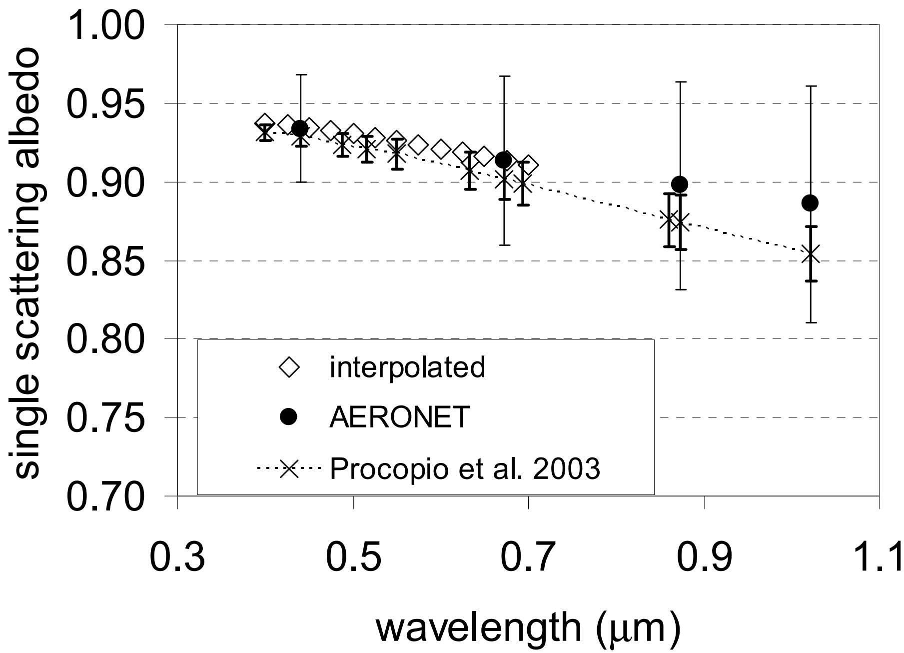

Fig. 1. Single scattering albedo in the PAR spectral range interpolated according to Mie theory (open diamonds). Solid black dots correspond to mean values from AERONET retrievals at 0.44, 0.67, 0.87 and 1.02 μm and standard deviation (an indication of data variability). Mean values from Procopio et al. (2003) are also shown for comparison (crosses).

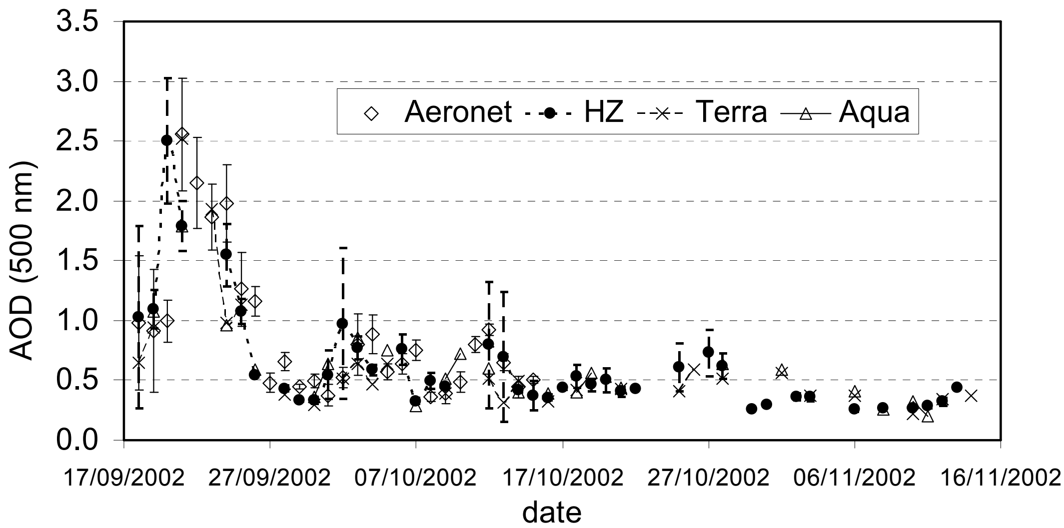

Fig. 2. Daily mean aerosol optical depth (AOD) at 500 nm observed at Rebio Jaru from 17 September to 15 November 2002. Results include AOD retrievals from AERONET (open diamonds), portable sunphotometer, HZ, (solid circles), MODIS aboard Terra (cross) and Aqua (open triangle) satellites. Vertical bars illustrate daily variability.

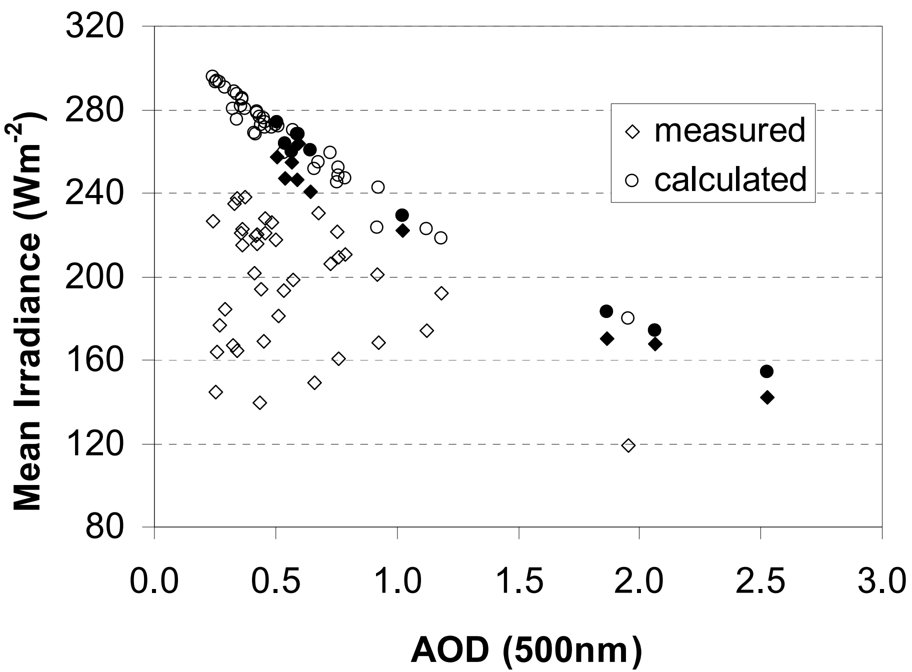

Fig. 3. Daily mean downward PAR irradiance at the top of the canopy at Rebio Jaru as function of AOD at 500 nm. Open symbols represent all analyzed data and solid symbols indicate situations when the effect of clouds was not significant.

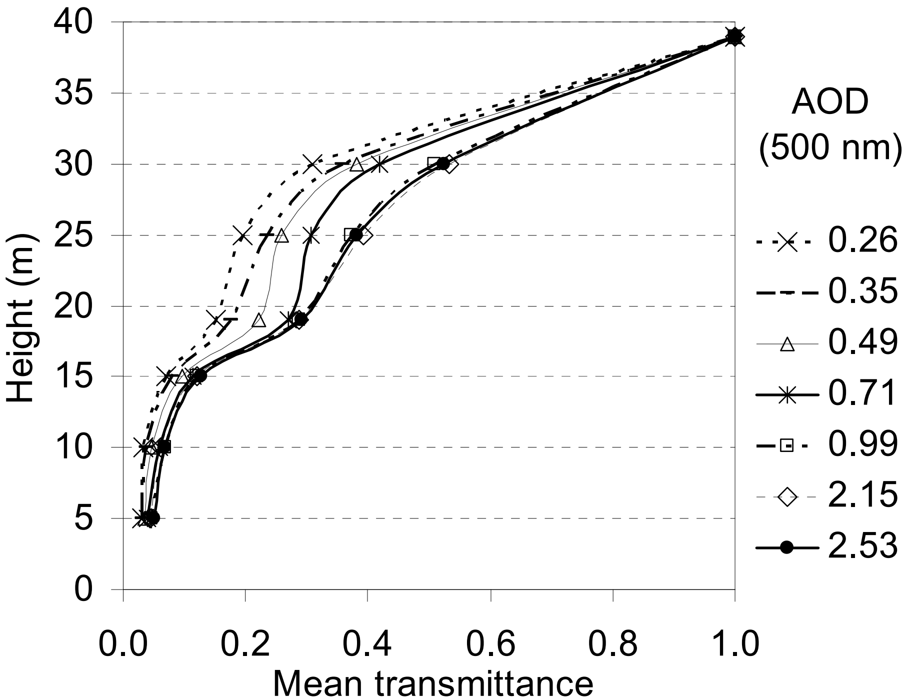

Fig. 4. Mean transmittance of photosynthetically active radiation inside the canopy at Rebio Jaru for distinct aerosol optical depths at 500 nm.

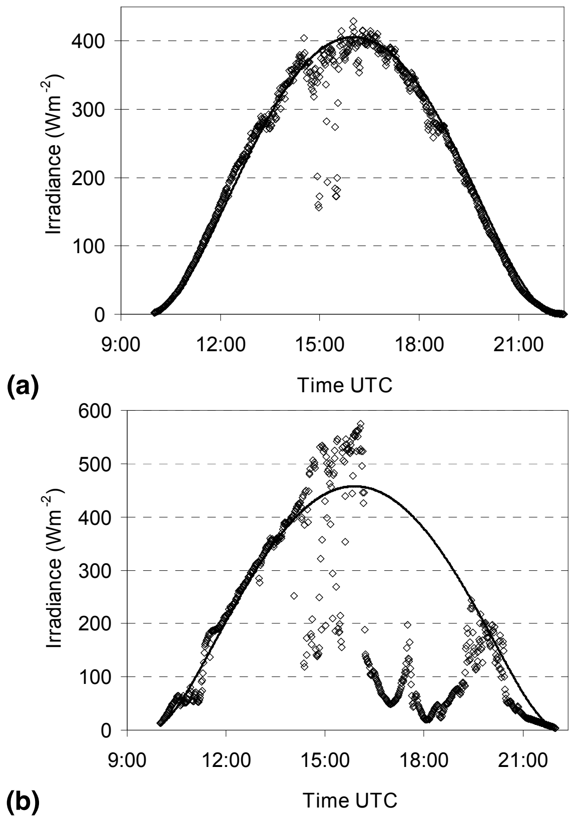

Fig. 5. Comparison of measured (open diamond) and calculated (solid curve) downward PAR irradiance at the top of canopy for **(a)** Cloud-free case on 20 September when mean AOD at 500 nm was 1.02±0.07 and the difference between daily mean measured and calculated PAR was 3.1% and **(b)** Cloudy case on 20 October when AOD at 500 nm was 0.51±0.07 and the difference between daily mean measured and calculated PAR was 50%.

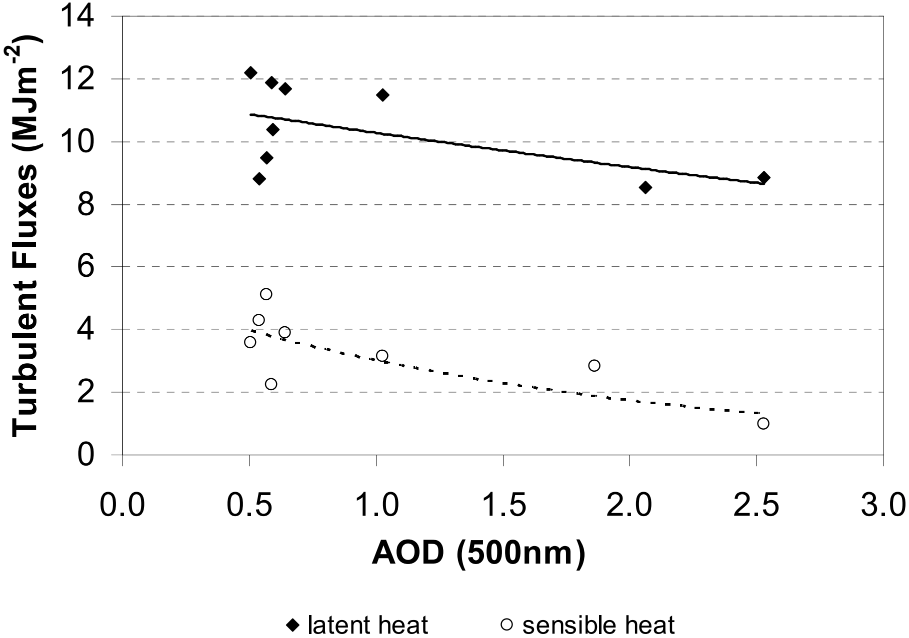

Fig. 6. Turbulent fluxes integrated from sunrise to sunset as function of daily mean AOD at 500 nm.

ACPD

5, 5909–5934, 2005

Title Page

Abstract | Introduction

Conclusions | References

Tables | Figures

◀ | ▶

◀ | ▶

Back | Close

Full Screen / Esc

Print Version

Interactive Discussion

EGU

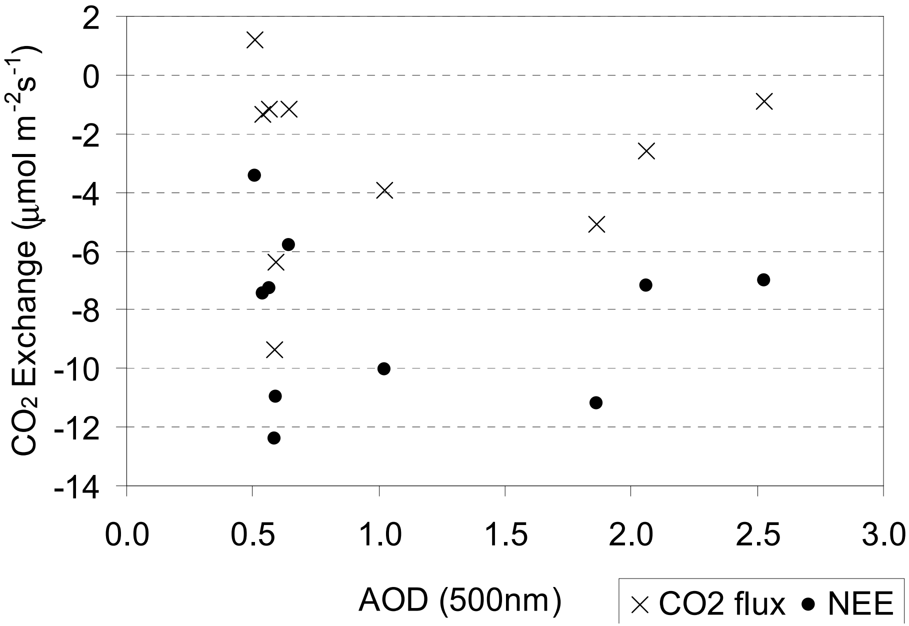

Fig. 7. Daily mean CO_2 exchange (CO_2 flux and NEE) from sunrise to sunset as function of daily mean AOD at 500 nm.

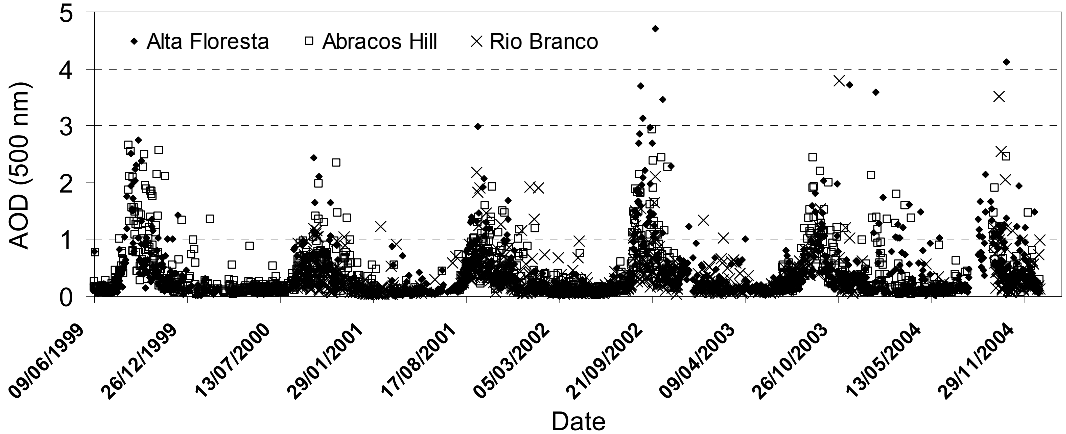

Fig. 8. Daily mean aerosol optical depth at 500 nm observed at Alta Floresta, MT, Abracos Hill, RO, and Rio Branco, AC. Alta Floresta is located in a region of transition vegetation from tropical rain forest to cerrado, Abracos Hill is located at a pasture site and Rio Branco is located in the Western portion of Amazon Basin in a region where tropical rain forest is the predominant vegetation.

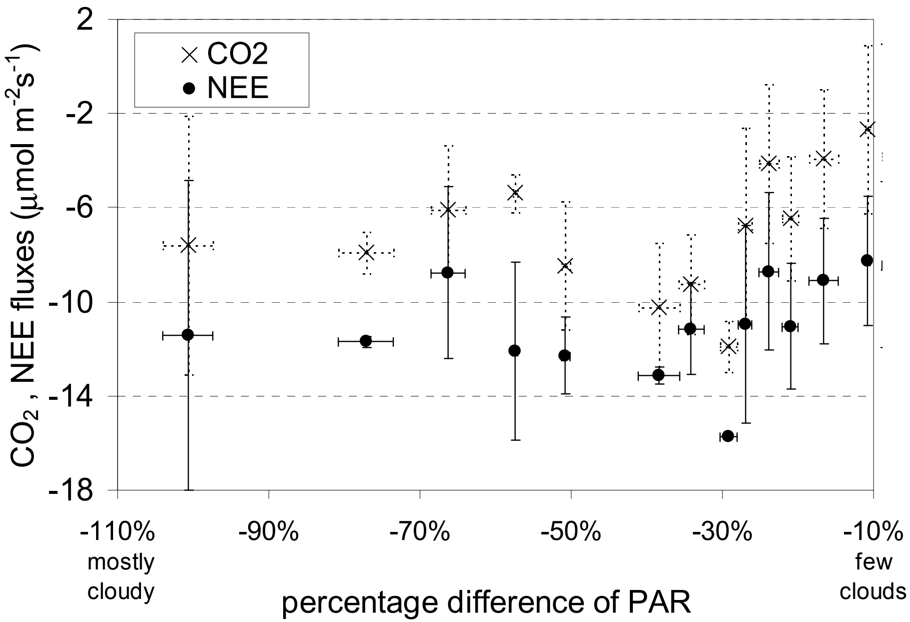

Fig. 9. Daily mean CO_2 and NEE fluxes from sunrise to sunset as function of percentage difference between measured and calculated daily mean downward global PAR irradiance at the top of the canopy. As discussed in the text, this percentage was a proxy for cloudiness, i.e., used to infer the presence of clouds at the site, thus, the more negative the value, more important is the effect of cloud cover on downward irradiance as compared to the aerosol radiation attenuation. Fluxes were averaged out according to bin intervals of PAR relative difference. Vertical and horizontal bars indicate variability of the data (one standard deviation).